

# Development of Active-Smart Packaging: Effect of Chitosan Nanofiber, Zinc Oxide Nanoparticles, and Anthocyanin on Gelatine-Based Halochromic Film for Meat Preservation

Nita Kusumawati<sup>1</sup>, Asrul Bahar<sup>2,\*</sup>, Maria Monica Sianita Basukiwardojo<sup>1</sup>, Samik<sup>1</sup>, Nunik Tri Rahayu<sup>1</sup>, Indri Wasa Estiningtyas<sup>1</sup>, & Muhammad Ridho Hafid Kurniawan<sup>1</sup>

<sup>1</sup>Department of Family Welfare Education, Universitas Negeri Surabaya, Jalan Ketintang, Ketintang, Kec. Gayungan, Surabaya, 60231, Indonesia

<sup>2</sup>Department of Chemistry, Universitas Negeri Surabaya, Jalan Ketintang, Ketintang, Kec. Gayungan, Surabaya 60231, Indonesia

\*Corresponding author: asrulbahar@unesa.ac.id

## Abstract

Gelatine-based smart active packaging has the potential to improve the quality of packaged meat and monitor its freshness without having to open it. This research aims to develop halochromic films by combining gelatine films with chitosan nanofibers (CHNF) and zinc oxide nanoparticles (ZnONPs). The addition of nanofillers such as CHNF and ZnONPs has been proven to improve mechanical properties (The humidity decreased by approximately 15.6%, while Young's modulus increased tenfold) and provide active packaging properties, such as antioxidants (IC50 test decreased 13% from 33,12191 to 28,82021) and antimicrobials against *S. aureus* (increased from 9,40 to 19.73 for inhibition zone), *E. coli* (increased from 6.61 to 19.91 of inhibition zone), and *P. aeruginosa* (increased from 8.63 to 18.65 of inhibition zone). Meanwhile, the smart packaging properties are provided by anthocyanin from telang flowers, which can change color as the freshness of the meat decreases or the acidity of the meat changes. The quality of smart active packaging is reflected in the pH sensitivity, ammonia release, and anthocyanin release. The film's mechanical properties also showed improvement in humidity, Young's modulus, water vapor permeability (WVP), and water solubility. Fourier Transform Infra-Red (FTIR) characterization analysis showed good compatibility between the gelatine, anthocyanins, CHNF, and ZnONPs matrix. This research result demonstrates that gelatine-based films with a combination of CHNF and ZnONPs can be used to create eco-friendly and multifunctional packaging films for meat preservation.

**Keywords:** *anthocyanin; chitosan nanofiber; clitoria ternatae; gelatine; packaging; zinc oxide nanoparticles.*

## Introduction

The World Health Organization (WHO) reports that more than 200 diseases, from diarrhea to cancer, arise from spoiled food, mainly due to the activity of foodborne pathogenic bacteria, namely *S. Aureus*, *E. Coli* and *P. Aeruginosa* (Bari & Kindzierski, 2018). These bacteria are the most common pathogens in the food industry, especially beef and its processed products, which are ideal media for pathogens due to high levels of protein, fat and water (Abebe, 2020). These pathogenic bacteria are generally difficult to penetrate synthetic plastic packaging, but environmental issues limit their wider use. This is the background for the development of biodegradable packaging.

Gelatine is one of the biodegradable packaging materials because it has good mechanical, thermal, and optical properties, and can form transparent and flexible thin film (Zulkiflee & Fauzi, 2021). However, gelatine also has disadvantages, such as being easily soluble in water, susceptible to microbes, and less compatible with other materials (Lu et al., 2022; Luo et al., 2022). To overcome these shortcomings, previous studies combined gelatine with chitosan which has unique properties such as non-toxicity, biocompatibility, biodegradability, excellent film-forming properties (Fernández-Marín et al., 2022). However, chitosan-based film packaging has weak antimicrobial activity and low mechanical properties (Alizadeh-Sani et al., 2020; Fernández-Marín et al., 2022). The application of nanofiber technology in this study is predicted to increase antioxidant, antimicrobial and nutraceutical activities as the surface area of chitosan increases, but despite being a good oxygen barrier, its moisture properties still need to be improved (Hajji et al., 2021).

The use of inorganic materials such as non-toxic zinc oxide nanoparticles (ZnONP) with high photocatalytic and antimicrobial activity stability is a potential solution to this problem. Although it has good antimicrobial properties, CHNF which is an organic material is still weak compared to inorganic materials such as ZnONPs which are more stable and have a high surface/volume ratio as surface reactivity increases, thus improving the mechanical and barrier properties of the film (Javed et al., 2020; Rahman et al., 2018). Thus, the application of Gelatine-CHNF-ZnONP (G-CZ) biodegradable packaging can have a synergistic effect on antimicrobial activity as well as mechanical properties.

The current demands of biodegradable packaging technology must have an effective way without having to open the packaging to determine the quality of the packaged food. Smart packaging technology is a new innovative food packaging technology that contains external materials or internal indicators to provide information about the status or quality of food without the need to damage the packaging (Drago et al., 2020). The application of smart packaging is designed to generate real-time signals in response to changes in food quality or external stimuli, one of which is changes in pH. Several studies report the use of synthetic coloring materials as colorimetric indicators that react directly to changes in pH in food, so that consumers can distinguish between fresh and rotten food without opening the package (Ma et al., 2021; Firouz et al., 2021). However, the development of smart packaging materials with colorimetric sensors based on toxic and carcinogenic synthetic dyes has triggered concerns about negative health impacts (Saliu & Della Pergola, 2018; Zhang et al., 2020).

Therefore, this study used dye sources as halochromic sensor materials. One of them is anthocyanin, a bioactive compound known for its high antioxidant and antimicrobial activities. Furthermore, the sensitivity to pH value makes this pigment not only a potential component in active packaging but can also be used as a color indicator that is responsive to pH changes (Moustafa et al., 2019). As a leading provider of anthocyanins, the blue petals of *Clitoria ternatea* not only have the ability to provide antioxidant and antimicrobial properties as active packaging, its broader utilization can be used as a pH-sensitive indicator that can provide changes in food freshness in smart packaging. So far, there has been no utilization of halochromic indicators from anthocyanins of *Clitoria ternatea* flowers as smart active packaging for fresh meat preservation.

## Material and Method

### Materials

The materials and their specifications used in this study were commercial cowhide B-type gelatine (225 g bloom), NaOH 30%, HCl 0.1 N, Tashiro indicator, HCl 25%, distilled water PE (Petroleum ether), HCl 3%, NaOH 30%, Litmus paper, PP indicator, Na<sub>2</sub>CO<sub>3</sub>, Citric acid, CuSO<sub>4</sub>·5H<sub>2</sub>O, H<sub>2</sub>SO<sub>4</sub> 25%, CH<sub>3</sub>COOH 3%, Glycerol (≥99.5%), calcium sulfate dihydrate (CaSO<sub>4</sub>·2H<sub>2</sub>O) (99%), calcium nitrate tetrahydrate (Ca(NO<sub>3</sub>)<sub>2</sub>·4H<sub>2</sub>O, 99%), potassium sulfate (K<sub>2</sub>SO<sub>4</sub>) (99%), polyvinyl alcohol (PVA; Sigma-Aldrich) - Singapore, CHNF (BCB-Chitin; 99%) - China, ZnONPs powder average particle diameter: 20–30 nm; 95%). (Reaching Biochemical Co.) – China.

### Butterfly pea flower extraction

The percolation or soaking procedure is used to extract butterfly pea flowers. Distilled water was used to extract dried butterfly pea flowers, which were ground with 1:6 (w/v) ratio for 30 minutes. After the extraction process is complete, the material is filtered using filter paper (Whatman No. 1). At a temperature of 37°C, anthocyanin extract from butterfly pea flowers was condensed using a rotary evaporator.

### Making CHNF

Electrospinning techniques were used to make chitosan/PVA nanofibers[49]. The magnetic stirrer was used to dispersed the PVA, which weighed 1.5 g, in 15 mL of pure water at a speed of 700 rpm (80 °C; 90 minutes) to produce a 10% PVA solution. To proceed further, we need to create a 3% chitosan solution. For this, 0.3 grams of chitosan powder should be added to 10 ml of acetic acid (CH<sub>3</sub>COOH) and stirred using a magnetic stirrer at a speed of 350 rpm (50 °C; 120 minutes). Both solutions were stored for 17 hours and then mixed for 20 minutes with a magnetic stirrer. The solution was ejected into the collection drum utilizing a Nacriebe 601 electrospinning tool at a range of 10 cm (flow rate 5 mL/hour; voltage 20 kV).

## Preparation of CHNF Solution

To make a CHNF solution, dispersed the CHNF with 0.04 g, in 2.5 g acetic acid 2% solution.

## Preparation of ZnONPs

Similarly, for the ZnONPs solution, dispersed ZnONPs weighing 0.3 g, in 2.5g acetic acid 2% solution. It was then stirred at a speed of 750 rpm (100 °C; 360 minutes) with a magnetic stirrer.

## Gelatine nanofiber Fabrication

To make gelatine nanofibers, two main ingredients were used: 10% gelatine with distilled water as a solvent and 12% PVA using 2% acetic acid as a solvent. The gelatine and PVA with a ratio of 1:2 was mixed for 20 minutes and then incubated at 20-25 °C for 17 hours. was ejected into the collection drum utilizing electrospinning at a range of 10 cm (flow rate 5 mL/hour; voltage 20 kV)

## Fabrication of composite films based on butterfly pea flower anthocyanin

Several ingredients such as Gelatine nanofiber, CHNF, ZnONP, glycerol, and anthocyanin extract were mixed with variations in composition depending on Table 1 in composition and factorial degassing for 15, 30, and 45 minutes. The film solution was homogenized with a magnetic stirrer at 350 rpm and a temperature of 25 °C for 60 minutes. The film solution was degassed at 30°C in a sonicator with 80 hz ultrasound-assisted homogenized to remove air bubbles contained in the solution. After sonication, the film solution was printed into acrylic measuring 20 x 20 cm with a thickness of 1.4 mm using the casting knife method. The film solution incubates at 20-25 °C for 3 days, then conditioned in a desiccator with 50% RH at 20-25 °C for 3 days. The film can be applied as meat packaging, with the following sample code in Table 1.

**Table 1** Sample Code for Variation Halochromic Film Composition

Degassing (minute)	Gelatine	Gelatine + ZnONPs	Gelatine + CHNF	Gelatine + CHNF + ZnONPs
15	G_I	G-Z_I	G-C_I	G-CZ_I
30	G_II	G-Z_II	G-C_II	G-CZ_II
45	G_III	G-Z_III	G-C_III	G-CZ_III

## DPPH Methods

The DPPH antioxidant activity assay begins with the preparation phase where 0.1 mM DPPH solution is prepared in methanol, followed by preparing varying concentrations of dispersed of film sample ranging from 20-100 µg/mL, with all solutions being protected from light exposure. The reaction phase involves taking 1 mL of each concentration of anthocyanin extract and combining it with 3 mL of the prepared 0.1 mM DPPH solution. This mixture is thoroughly homogenized using a vortex mixer and then incubated in dark conditions at room temperature for a duration of 30 minutes. Following incubation, the measurement phase is conducted where the absorbance is measured at 517 nm using a UV-visible spectrophotometer, with methanol serving as the blank. A control sample is prepared by substituting the extract with 1 mL of methanol. The antioxidant activity is then quantified by calculating the percentage of DPPH radical scavenging activity using the formula: DPPH scavenging activity (%) = [(Ac - As)/Ac] × 100, where Ac represents the absorbance of control and As represents the absorbance of sample.

## Result and discussion/Result

### Moisture on Films

Moisture testing is an important requirement for packaging materials. A complex structure of polymers and/or nanoparticles interlock to form packaging materials. The structure contains tiny spaces where water molecules and other substances are confined (Musso et al., 2019). Moisture testing has been carried out on 12 samples of halochromic film packaging with the data in Table 2. Additives are added to the film for decreases the water content, with an increase in certain additives, especially ZnONPs, causing the water content in the film to become lower as shown at Table 2, the lowest water content was recorded in film samples with the addition of ZnONPs. The positive correlation between the water content in the film packaging with the WVP value > water content. Films made from

biopolymers are often found to have this issue, which is commonly reported, as compared to those made from synthetic polymers (Dodero et al., 2021).

**Table 2** Moisture Test of Halocromic Film

Sample	Moisture Absorbtion (%)	STD Deviation
G_I	8,2167	± 0,130
G_II	8,4424	± 0,102
G_III	8,7133	± 0,103
G-Z_I	7,3929	± 0.121
G-Z_II	7,5729	± 0.136
G-Z_III	7,6238	± 0.132
G-C_I	7,3519	± 0.094
G-C_II	7,3538	± 0.118
G-C_III	7,3849	± 0.087
G-CZ_I	7,4129	± 0.101
G-CZ_II	7,5238	± 0.087
G-CZ_III	7,6749	± 0.098

The moisture absorption data presented in Table 2 reveals significant variations across different film compositions and their modifications. Pure gelatine films (G\_I, G\_II, G\_III) demonstrate the highest moisture absorption values ranging from 8.2167% to 8.7133%, showing an increasing trend from G\_I to G\_III. This high moisture absorption is attributed to gelatine's inherently hydrophilic nature, which stems from its numerous -OH and -NH<sub>2</sub> groups, open protein structure, and abundant hydrogen bonding sites.

The film samples absorbed less moisture when more ZnONPs additive was added (G-Z\_I, G-Z\_II, G-Z\_III), and this difference was significant ( $p < 0.05$ ). The moisture percentage value for the G-Z sample is 7.39% (I); 7.57% (II); 7.62% (III) after 96 hours. This reduction occurs because ZnO nanoparticles occupy intermolecular spaces and form coordination bonds with gelatine's functional groups, thereby reducing the availability of hydrophilic groups for water interaction.

Similarly, the gelatine-chitosan films (G-C\_I, G-C\_II, G-C\_III) exhibit reduced moisture absorption (7.3519% - 7.3849%) with remarkably stable values across variations, attributed to chitosan's crystalline structure, the formation of intermolecular hydrogen bonds between gelatine and chitosan, and the creation of a more compact network structure.

Meanwhile, the moisture percentage for the G-CZ film is 7.41% (I); 7.52% (II); 7.67% (III), which is significantly less moisture than other film samples. with a gradual increasing trend, explained by complex interactions between all three components, ZnONPs can improves the gelatine structure's ability to resist water by creating some discontinuities in the G-C network, and a balanced effect of hydrophobic and hydrophilic interactions. Overall, the moisture absorption follows the order:  $G > G-CZ > G-Z \approx G-C$ , indicating that the addition of both chitosan and ZnO helps create more moisture-resistant films by reducing available sites for water molecule interaction and creating a more stable network. These findings are particularly significant for packaging applications requiring moisture resistance, storage stability, potential use in humid environments, and overall film durability and performance. The research conducted by Roy (2022) supports this discovery, the integration of ZnONPs can reduce the value of moisture absorption in bacterial cellulose-based films through the formation of new interactions and stronger structures (Roy et al., 2022).

Addition of CHNF also have advantages for active film. CHNF is a nanofiber derived from chitin, a polysaccharide found in the shells of marine animals (Hai et al., 2020). CHNF has antibacterial, biocompatible, and biodegradable properties, which can help maintain the quality and freshness of films. Moreover, CHNF can improve the transparency and mechanical strength of films, which can reduce the moisture absorption (Heidari et al., 2021). The variations 7 to 12 in the table above demonstrate the relevance of the theory. These films, which contain CHNF, have lower moisture levels compared to films without CHNF. This indicates that smart active films perform better. The films have less empty space and stronger bonds between molecules because of this network structure (Roy et al., 2021). CHNF can also act as a filler, The films can have their porosity and water vapor permeability reduced through the use of a specific method or substance. This means that CHNF can prevent the water molecules from entering or leaving the films, which lowering the film moisture (Amjadi et al., 2019).

## FTIR

The halochromic film's chemical composition was determined by performing FTIR analysis has shown at Figure 1. Glycerol interaction was observed in all of the nanocomposite films, it was observed at 1033.16  $\text{cm}^{-1}$  (G); 1031.59  $\text{cm}^{-1}$  (G-C); 1034.33  $\text{cm}^{-1}$  (G-Z); and 1034.64  $\text{cm}^{-1}$  (G-CZ). These peaks in the 1030-1035  $\text{cm}^{-1}$  region typically correspond to the C-O stretching vibrations and are characteristically associated with chitosan's structure. The peak shifts observed in the various combinations (G-C, G-Z, G-CZ) compared to plain gelatine (G) suggest significant interactions with the chitosan component, particularly in the region associated with the pyranose ring C-O stretching in chitosan's structure. Among the four materials mentioned (gelatine, chitosan, zinc oxide, and anthocyanin), these peaks around 1031-1035  $\text{cm}^{-1}$  primarily indicate the presence and interactions of chitosan in the various combinations. This observation is supported by several key findings: plain gelatine (G) shows the base peak at 1033.16  $\text{cm}^{-1}$ , and when chitosan is added (G-C), a shift to 1031.59  $\text{cm}^{-1}$  is observed. Furthermore, combinations with zinc oxide (G-Z and G-CZ) demonstrate shifts to slightly higher wavenumbers (1034.33 and 1034.64  $\text{cm}^{-1}$ ). While these shifts suggest molecular interactions between the materials, the fundamental peak in this region is primarily associated with chitosan's C-O stretching vibrations, indicating its significant role in the molecular structure of these combinations.

Absorption peaks at wavelengths of 1033 - 1035  $\text{cm}^{-1}$  were found in the G-Z and G-CZ film variations, this is related to the connection between OH groups found in glycerol and gelatine, these peaks indicate that ZnONPs successfully mixes with the film, forming a matrix of gelatine and glycerol (Bahar et al., 2023).

Interactions derived from gelatine are shown at wave numbers in the range 1450-1630  $\text{cm}^{-1}$  that represent to amide, carbonyl, and methylene bonds. The O-H bending bond derived from glycerine can be look at the range of 920 - 922  $\text{cm}^{-1}$  (Moustafa et al., 2019). All composite films in Figure 1. show similar specific peaks: 1) amide-A band at 3279.45 - 3286.82  $\text{cm}^{-1}$  which also indicates secondary amine groups; and 2) amide-B band at 2924.13 - 2931.12  $\text{cm}^{-1}$ . Amide-(I, II, and III) have distinct peaks at 1630.33 - 1633.78  $\text{cm}^{-1}$ ; 1538.29 - 1539.09  $\text{cm}^{-1}$ ; 1236.93 - 1238.77  $\text{cm}^{-1}$ , respectively, these peaks are also present in all films.

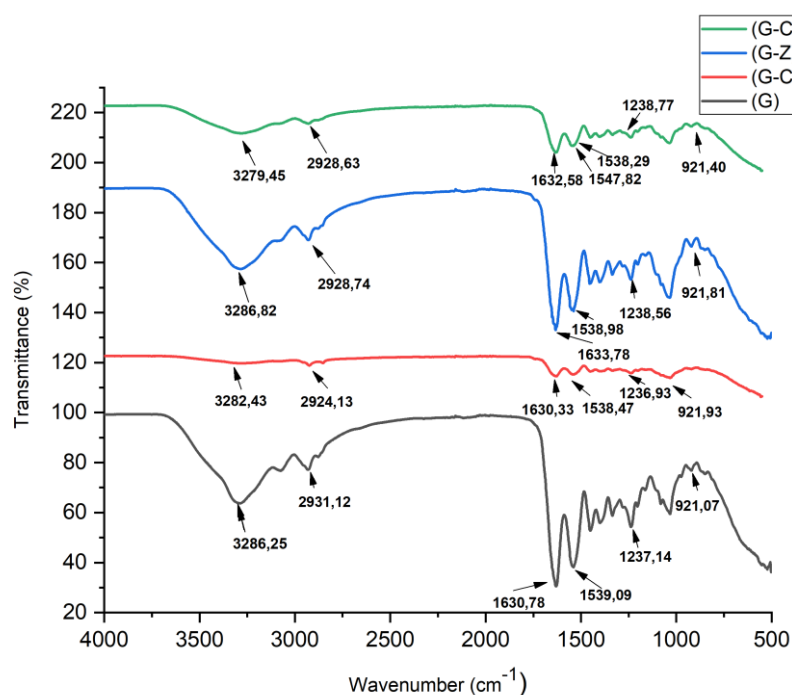


**Figure 1** FTIR graphic of all nanocomposite films.

Incorporating CHNF during the electrospinning process leads to modifications in wave numbers for amide-(I, II, and III). This is attributed to the development of intramolecular hydrogen bonds in chitin. The group of N-H in gelatine and ZnONPs formed hydrogen bonds that caused a shift, which was also due to the ZnONPs (Bahar et al., 2023). The gelatine polypeptide chain's structure changed because of CHNF and ZnONPs, which reduced the number of single  $\alpha$ -helices, random coils, and irregular structures. This change was confirmed by a reduction in peaks at 1547.82 and 1538.29  $\text{cm}^{-1}$ . Gelatine contains groups such as -OH, -COOH, and -NH<sub>2</sub>, which can form hydrogen bonds with group of -OH and -

NH<sub>2</sub> that are in CHNF and ZnONPs (Jiao et al., 2020). The bands related to amino, amide, and hydroxyl group showed a small change in the G-CZ film spectrum, indicating a connection between gelatine, CHNF, and ZnONPs.

## Antioxidant Activity

The antioxidant activity of active-smart packaging will be measured by the DPPH method. This experiment was done to find out the antioxidant activity in the butterfly pea flower anthocyanin extract. Anthocyanins, which are flavonoids that trigger red, blue, purple and orange colors, not only have potential as active packaging materials but also as smart packaging sensors. The butterfly pea flower, also known as *Clitoria ternatea*, produces blue petals that are rich in anthocyanins and in fact it is the largest source of them, these anthocyanins are highly regarded for their bioactivity and safety when consumed (Alizadeh-Sani et al., 2021; Alizadeh-Sani et al., 2021; Arifin et al., 2021). This research will test the use of anthocyanins as health and environmentally friendly colorimetric sensors for active-smart packaging materials that have potential to preserving fresh beef.

All the samples in the provided Table 3 have an antioxidant activity value (IC<sub>50</sub>) less than 50, as can be observed from the table. In accordance with the IC<sub>50</sub> value parameters from Table 3., this shows that butterfly pea flower petals (*Clitoria ternatea*) are a very strong antioxidant (IC<sub>50</sub> value <50). In the gelatine composition with a degassing variation of 15 minutes, the highest IC<sub>50</sub> antioxidant activity value was obtained compared to the 30 minute and 45 minutes degassing variation. IC<sub>50</sub> of the film can be influenced by the duration of degassing. The DPPH antioxidant activity results presented in Table 3 show that all samples have IC<sub>50</sub> values less than 50, which indicates strong antioxidant activity since a lower IC<sub>50</sub> value represents higher antioxidant capacity. The degassing time appears to positively influence the antioxidant activity, as evidenced by the decreasing IC<sub>50</sub> values with longer degassing times. This suggests that the degassing process may help in better extraction or preservation of antioxidant compounds, thereby enhancing their ability to scavenge free radicals. This enhancement in antioxidant activity could be attributed to improved accessibility of the active compounds or potential structural modifications during the degassing process that favor better radical scavenging capacity (Erdem & Kaya, 2022).

**Table 3** Antioxidant activity of halochromic film

Sample	Antioxidant Activities (IC <sub>50</sub> )	STD Deviation
G_I	33,12191	± 0,11583
G_II	33,51891	± 0,15741
G_III	33,51121	± 0,07234
G-Z_I	31,21431	± 0,12741
G-Z_II	31,91566	± 0,22663
G-Z_III	32,82021	± 0,17741
G-C_I	29,12110	± 0,12223
G-C_II	29,21160	± 0,16183
G-C_III	29,73140	± 0,24183
G-CZ_I	29,12191	± 0,07550
G-CZ_II	29,11916	± 0,15741
G-CZ_III	28,82021	± 0,12183

The enhanced IC<sub>50</sub> antioxidant activity values observed in compositions containing Gelatine + ZnONPs, Gelatine + CHNF, and Gelatine + CHNF + ZnONPs at 45 minutes degassing time compared to 15 and 30 minutes can be explained through several mechanisms. The primary mechanism involves ZnONPs' electron transfer properties, where these nanoparticles act as electron donors due to their semiconductor characteristics. Specifically, the conduction band electrons (e<sup>-</sup>) of ZnO can interact with oxygen molecules to form superoxide radicals (O<sub>2</sub><sup>•-</sup>), which can further react with H<sup>+</sup> to form hydrogen peroxide (H<sub>2</sub>O<sub>2</sub>), ultimately enhancing the overall redox activity and free radical scavenging capacity. The surface area effect also plays a crucial role, as longer degassing time (45 minutes) likely improves the dispersion of ZnONPs, leading to increased effective surface area for antioxidant reactions and providing more active sites for free radical scavenging. Additionally, synergistic interactions occur during the extended degassing time, allowing for better molecular interactions between ZnONPs and gelatine's amino groups (-NH<sub>2</sub>), as well as ZnONPs and CHNF's hydroxyl groups (-OH), creating a more stable network with improved electron-donating capability.

From the data shown in the Table 3, it is found that the addition of CHNF to the film can increase antioxidant activity. The results of testing antioxidant activity on a variety of films with the addition of CHNF showed that the antioxidant value was lower, this shows that the antioxidant activity is stronger. The addition of CHNF can increase antioxidant

activity because CHNF contains compounds that have hydroxyl and carbonyl groups which can interact with free radicals (Barman et al., 2020). Apart from that, the addition of ZnONPs to the film can also increase antioxidant activity because ZnONPs is a zinc oxide nanoparticle which has photocatalytic properties and can ward off free radicals.

## Modulus Young

The composition of bioplastics affects their mechanical properties, including Young's modulus. According to Nandiwilastio (2019), the Young's modulus value is always inversely proportional to the elongation of the material when tested in tension. In other words, if a bioplastic has a low Young's modulus, then it is likely that the material is flexible. This can be seen from the significant increase in length when the material is pulled, through the elastic region, and does not return to its original length (Nandiwilastio et al., 2019).

As shown in Table 4, the G-Z film has a higher Young's modulus value than the G film, which does not have ZnONPs. Tests on film samples with the highest gelatine composition produced a Young's modulus value of 81.98 MPa, while on film samples with the highest addition of ZnONPs it reached 3231.29 MPa. This finding can be explained by the reason for this result is that ZnONPs particles can spread well in the matrix, which helps them to hold more polymer chains, it was through two main mechanisms: the interfacial bonding mechanism and physical interactions. In the interfacial bonding mechanism, ZnONPs contain Zn<sup>2+</sup> ions on their surface that act as Lewis acids, capable of forming coordination bonds with -NH<sub>2</sub> groups from gelatine, -OH groups from chitosan, and -COOH groups from gelatine. The physical interactions involve Van der Waals forces between ZnONPs and polymer chains, hydrogen bonding between surface -OH groups of ZnONPs and polymer functional groups, and electrostatic interactions between charged surfaces. The mechanism progresses through several key steps, beginning with initial dispersion where ZnONPs disperse throughout the polymer matrix during mixing, while the degassing process helps remove air bubbles and improve dispersion. This is followed by surface interaction, where the surface of ZnONPs presents multiple binding sites and polymer chains approach and begin interacting with these sites. During bond formation, coordination bonds form between Zn<sup>2+</sup> and electron-rich groups, allowing multiple polymer chains to attach to a single ZnONP due to its high surface area, while cross-linking occurs between different polymer chains through the ZnONP. Finally, network stabilization occurs as the formed network is stabilized by multiple attachment points per ZnONP, varied types of bonds, and physical entanglement of polymer chains. This comprehensive mechanism explains why well-dispersed ZnONPs can hold more polymer chains through multiple binding sites, high surface area to volume ratio, various types of possible interactions, three-dimensional network formation capability, and enhanced cross-linking potential. The resulting structure creates a more stable and robust polymer network with improved mechanical and physical properties (Chen et al., 2022).

**Table 4** Modulus Young of Halochromic Film

Sample	Modulus Young (MPa)	STD Deviation
G_I	78,59	± 0,46
G_II	81,98	± 0,79
G_III	79,31	± 0,61
G-Z_I	3198,09	± 1,52
G-Z_II	3231,29	± 2,25
G-Z_III	2976,45	± 2,27
G-C_I	133,892	± 0,855
G-C_II	152,44	± 1,3
G-C_III	119,87	± 1,31
G-CZ_I	876,431	± 1,589
G-CZ_II	935,09	± 2,21
G-CZ_III	799,091	± 1,989

ZnONPs interact with gelatine and chitosan through two main mechanisms: interfacial bonding and physical interactions. The Zn<sup>2+</sup> ions on the surface of ZnONPs form coordination bonds with the -NH<sub>2</sub> groups from gelatine, -OH groups from chitosan, and -COOH groups from gelatine. Physical interactions such as Van der Waals forces, hydrogen bonding, and electrostatic interactions also play a significant role. Initially, ZnONPs disperse throughout the polymer matrix during mixing, and the degassing process helps in removing air bubbles, which enhances dispersion. Then, polymer chains approach and interact with the multiple binding sites on the ZnONPs' surface. Coordination bonds form between Zn<sup>2+</sup> and electron-rich groups, leading to multiple polymer chains attaching to a single ZnONP due to its high surface area. Cross-linking occurs between different polymer chains through the ZnONP, creating a stabilized network due to multiple attachment points, varied types of bonds, and physical entanglement of polymer chains. This mechanism results in a more stable and robust polymer network with improved mechanical and physical properties.

The interactions within the matrix also increase, the film's mechanical properties were enhanced due to certain changes made. The reinforcement effectiveness of ZnONPs also contributes to increasing the Young's modulus value, where the dispersion and effectiveness of the reinforcement play a key role (Mohammed et al., 2023).

The G-C film with CHNF added demonstrates a higher Young's modulus value than the G-C film that lacks CHNF. This increase could be caused by an increase in the crystallinity of the film matrix triggered by the formation of an interconnecting pore network by CHNF (Chen et al., 2023). This creates stronger interfacial interactions, resulting in increased mechanical stability of the film. The result is supported by Zhang (2020) research, where the increase in young's modulus of G-C films is due to the formation of hydrogen bonds between chains. This causes stretch at polymer chains, which makes the edible film more elastic and compact (Bahar et al., 2023).

### Antimicrobial Activity

Each ingredient's antibacterial potential tested with disk diffusion assay. The two types of bacteria studied are gram-negative bacteria like *Escherichia coli* and *Pseudomonas aeruginosa* and gram-positive bacteria like *Staphylococcus aureus*. The diameter of the inhibition zone for each film sample against the bacteria can be found in Figure 2. And Table 5.

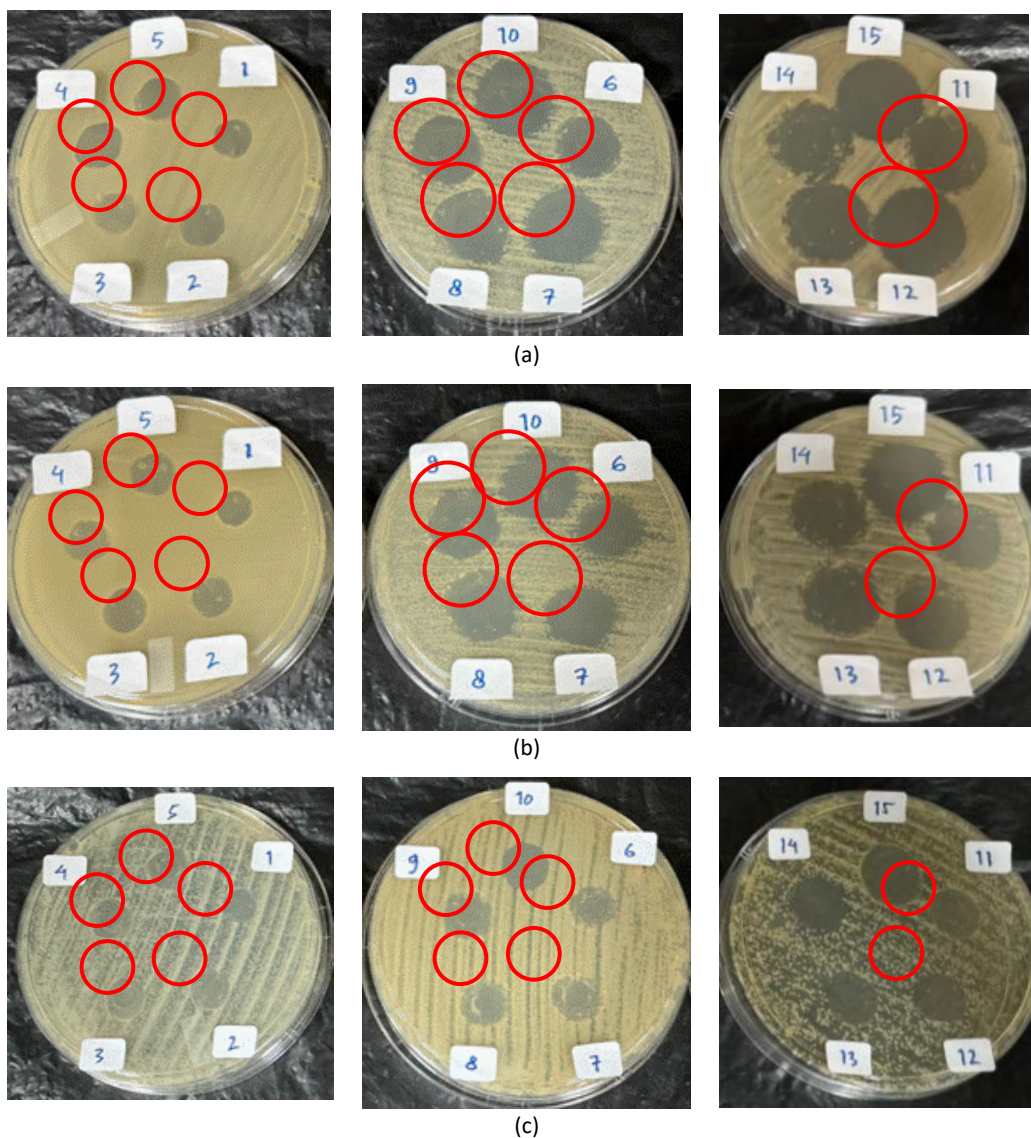


**Figure 2** The measurement of the inhibition zone of sample against the bacteria for (A) *S. aureus* [1-12], (B) *E. coli* [1-12], and (C) *P. aeruginosa* [1-12] bacteria



**Table 5** Antimicrobial Activity of Halochromic Film

Composition	Degassing (Minute)	<i>Staphylococcus aureus</i> (mm)	<i>Escherichia Coli</i> (mm)	<i>Pseudomonas aeruginosa</i> (mm)
G_I	15	9,40	6,61	8,63
G-C_I		9,83	10,26	9,21
G-Z_I		11,05	11,21	10,31
G-CZ_I		12,40	11,95	11,13
G_II	30	13,18	13,13	11,83
G-C_II		15,60	15,08	12,58
G-Z_II		16,63	16,78	13,58
G-CZ_II		17,31	17,45	14,71
G_III	45	17,68	17,75	15,63
G-C_III		18,88	18,65	16,6
G-Z_III		19,35	19,43	17,71
G-CZ_III		19,73	19,91	18,65

The data shown in Table 5 above leads to the conclusion that, in comparison to other samples, gelatine (G) films show less antibacterial activity. The G.C film exhibits zones of inhibition against *S. aureus*, *E. coli*, and *P. aeruginosa* with measurements of 8.18 mm, 10.68 mm, and 9.19 mm. However, because G.C. film exhibits inhibitory zones against the bacteria, which measure 8.18 mm, 10.68 mm, and 9.19 mm, respectively, it may be said that the bacteria are vulnerable to it. G.Z film demonstrates zones of inhibition measuring 11.65 mm, 10.38 mm, and 9.03 mm against the bacteria. Meanwhile, it's worth noting that the film also displays inhibitory effects.

The results show that the G.Z film is more effective in killing Gram-positive bacteria, especially *S. aureus*, than Gram-negative bacteria, such as *E. coli* and *P. aeruginosa*. The antimicrobial activity mechanism of ZnONPs involves the release of Zn<sup>2+</sup> ions, which can penetrate bacterial cell walls and cause bacterial death through reactions with the cytoplasm and oxidative stress that produces Reactive Oxygen Species (ROS) (Dzeikala et al., 2023; Ezati et al., 2019). However, because G.C. film exhibits inhibitory zones against the bacteria, which measure 8.18 mm, 10.68 mm, and 9.19 mm, respectively, it may be said that the bacteria are vulnerable to combination of gelatine and chitosan. This is due to the more complex cell wall structure of gram-negative bacteria, which has an outer membrane that can act as a barrier to keep ROS out. The incorporation of CHNF in gelatine films results in antimicrobial activity by means of the positively charged amino groups (NH<sub>3</sub><sup>+</sup>) from glucosamine. These groups interact with the negatively charged outer membrane of bacteria, creating pores that cause bacterial cell death (Huang et al., 2019). The antibacterial properties of the G-CZ film are considerably stronger when compared to those of the G-C and G-Z films used individually. The sizes of the inhibition zones against *S. aureus*, *E. coli*, and *P. aeruginosa* are 14.63 mm, 12.30 mm, and 11.15 mm, respectively.

These results indicate a synergistic effect between CHNF and ZnONPs in enhancing antimicrobial activity. Bacterial DNA may be harmed and eventually perish because CHNF amino group interactions to negatively charged cell membrane of bacteria. It can be concluded that gram-negative bacteria are more susceptible to the combined action of these factors. Thus, it can be concluded that the addition of CHNF does not reduce the antibacterial activity of ZnONPs but rather provides a synergistic effect that enhances the antimicrobial activity of ZnONPs. These findings support previous research reporting by Bahar (2023) that found similar effects with other nanoparticles in the presence of packaging material for cheddar cheese based on gelatine, chitosan nanofiber, and zinc oxide nanoparticles (G/CHNF/ZnONPs) (Bahar et al., 2023).

### Water Vapor Permeability (WVP)

WVP testing are performed to evaluate the degree of water vapor permeability of every packaging sample. If the WVP value is higher, then it implies that the quality of the packaging is lower because it gets more easily soaked by water vapor, as elaborated by the source (Jiao et al., 2020). The method used in this analysis is ASTM E 96-95 (Nandiwilastio et al., 2019). It is important for the packaging to have antimicrobial properties and to be able to regulate the permeability of gas and water vapor (Othman et al., 2023). Therefore, it is necessary to standardize the composition and degassing process on film samples to reduce water vapor permeability. The WVP test has been carried out on six of the total twelve samples available in Table 6.

**Table 6** WVP of halochromic film

Sample	WVP (g/m.h.Pa)	STD Deviation
G/I	$7.24116 \times 10^{-8}$	$\pm 0.08615$
G/II	$9.08243 \times 10^{-8}$	$\pm 0.08725$
G/III	$11.0661 \times 10^{-8}$	$\pm 0.11235$
G-C_I	$7.44126 \times 10^{-8}$	$\pm 0.08925$
G-C_II	$9.34217 \times 10^{-8}$	$\pm 0.09215$
G-C_III	$11.1815 \times 10^{-8}$	$\pm 0.08725$
G-Z_I	$7.14111 \times 10^{-8}$	$\pm 0.08525$
G-Z_II	$7.81259 \times 10^{-8}$	$\pm 0.08925$
G-Z_III	$10.9984 \times 10^{-8}$	$\pm 0.08615$
G-CZ_I	$6.81788 \times 10^{-8}$	$\pm 0.08725$
G-CZ_II	$7.78373 \times 10^{-8}$	$\pm 0.09015$
G-CZ_III	$9.29984 \times 10^{-8}$	$\pm 0.08825$

Table 6 Test results show that the WVP level in each film sample follows a similar pattern to the percentage of moisture absorption, with a significant increase ( $p < 0.05$ ) because CHNF addition. The WVP value increased from  $7.24 \times 10^{-8}$  to  $7.44 \times 10^{-8}$  g/m.h.Pa (I); from  $9.08 \times 10^{-8}$  to  $9.34 \times 10^{-8}$  g/m.h.Pa (II); from  $11.06 \times 10^{-8}$  to  $11.18 \times 10^{-8}$  g/m.h.Pa (III). Presence of CHNF in the films enhanced their hydrophilic properties by increasing the number of polar groups and O-H bands, which resulted in greater water diffusion. The findings are consistent with a study by Sahraee (2017), which found that adding chitin nanoparticles raised the WVP value of gelatine films. These nanoparticles possess hydrophilic properties of high intensity (Sahraee et al., 2017).

Hydrogen bonds were formed when ZnONPs were incorporated into gelatine, which reduced the free hydrophilicity of G-Z films. Consequently, a noteworthy decrease in WVP values ( $p < 0.05$ ) was observed in comparison to films devoid of ZnONPs. The nanocomposite film G-CZ exhibited a significantly lower ( $p < 0.05$ ) WVP value in comparison to the G and G-C films. Despite this, the G-Z film did not show a significant difference in its WVP value ( $p > 0.05$ ), which was measured to be  $6.81 \times 10^{-8}$  g/m.h.Pa (I);  $7.78 \times 10^{-8}$  g/m.h.Pa (II);  $9.29 \times 10^{-8}$  g/m.h.Pa (III). The addition of ZnONPs had a more significant impact on reducing WVP compared to CHNF. The gelatine structure might have less hydrophilic groups because of the hydrogen bonds that could form between the gelatine matrix and ZnONPs. This result is consistent with work by Shahmohammadi and Almasi (2016), who found that adding ZnONPs can increase resistance to water vapor by slowing down the movement of gelatine chains by filling the empty space between them (Shahmohammadi & Almasi, 2016).

## pH Sensitive

pH-sensitive markers that are dependent Food freshness may be promptly monitored using intelligent active packaging. Meat products can undergo significant pH fluctuations while being stored, which might reduce their freshness (Roy et al., 2022; Roy & Priyadarshi, 2021). pH measurements were performed on halochromic smart films that contained anthocyanins in this study. The film's color changes depending on the pH: it turns red or pink at pH values below 4, purple at pH values between 5 and 6, bluish-grey at pH values between 7 and 8, green at pH values between 10 and 12, and yellow at pH values above 12. Rose anthocyanins also reported have caused pH-induced color changes in PVA/okra slime composite films (Alizadeh-Sani et al., 2021; Sharaby et al., 2024; Kang et al., 2020).

**Table 7** pH sensitive test of halochromic film

Sampel	pH Sensitive
G_I	$5.30 \pm 0.01$
G_II	$5.32 \pm 0.01$
G_III	$5.35 \pm 0.01$
G-Z_I	$5.46 \pm 0.01$
G-Z_II	$5.53 \pm 0.01$
G-Z_III	$5.55 \pm 0.01$
G-C_I	$5.57 \pm 0.01$
G-C_II	$5.60 \pm 0.01$
G-C_III	$5.69 \pm 0.01$
G-CZ_I	$5.73 \pm 0.01$
G-CZ_II	$5.77 \pm 0.01$
G-CZ_III	$5.85 \pm 0.01$

One of the metrics that is frequently used to track changes in meat quality that are related to color, tenderness, flavor, water binding ability, and shelf life is acidity level (pH). Fresh meat has a pH value ranging from 5.3-5.9 (Qian et al., 2021). In pH 2, 7 and 12, the anthocyanin solution displayed colors ranging from blue to pink, green, and yellow (Sitanggang et al., 2020). Table 7 presents test results of pH sensitive.

### Anthocyanin Release

Smart packaging films have extensively utilized anthocyanins in their production. Incorporating anthocyanins into color indicator smart packaging films based on biodegradable polymer is beneficial for monitoring food freshness. Anthocyanins show remarkable properties such as being pH-sensitive, antioxidant, and antimicrobial (Soradech et al., 2017). Films with anthocyanin extract have lower brightness and yellowish color compared to films without anthocyanin extract as the data seen in Table 8 which also corresponds to the colors generated in Figure 3 (Wang et al., 2019).

**Table 8** Anthocyanin Release of Halochromic Film

Sample	Anthocyanin release ( $\mu\text{g} / \text{mm}^2$ )
G_I	0.53
G_II	0.50
G_III	0.45
G-Z_I	0.43
G-Z_II	0.41
G-Z_III	0.37
G-C_I	0.35
G-C_II	0.33
G-C_III	0.27
G-CZ_I	0.21
G-CZ_II	0.20
G-CZ_III	0.17

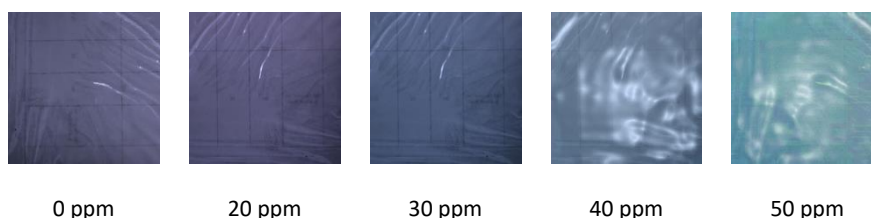


**Figure 3** Color Changes and Film Sensitivity to Ammonia Vapor of All Nanocomposite

### Ammonia Vapor Release

Color indicator films were exposed to ammonia vapor. This was done to evaluate the color changes of volatile nitrogen compounds. The goal was to make indicators/sensors that could be used to check the quality of foods that are rich in protein (Kang et al., 2020). The data displaying the effect of ammonia vapor on film sensitivity and color alteration is presented in Figure 3.

As anticipated, it shown obvious color change from dark blue to light blue during sensitivity testing using ammonia solution (NH<sub>4</sub>OH), which evaporates into ammonia gas (NH<sub>3</sub>) (Yong et al., 2019; Zhang et al., 2022). The freshness sensor membrane detects a gas and signals a change in its color. The image shows the color change on the freshness sensor at concentrations of 20, 30, 40, and 50 ppm after exposure to ammonia vapor (NH<sub>3</sub>). Three freshness sensors provide a clear and easily recognizable color change reaction visually at concentrations of 40 and 50 ppm. However, the time required for the color change varies at each concentration because the pH value is different at each concentration, so the response time is longer to respond to changes in pH due to ammonia vapor (NH<sub>3</sub>) from the ammonia solution (NH<sub>4</sub>OH).

As storage at room temperature becomes longer, there is an increase in the activity of microorganisms which produce more basic compounds. This can result in meat spoilage which can be observed through physical changes, such as color, texture and odor in the meat, which can be assessed through organoleptic tests. Overall, the research results show that

the developed anthocyanin-containing composite film has the ability to detect ammonia gas, indicating its sensitivity to changes in meat freshness.

## Water Solubility (WS)

The functional performance of packing materials is significantly influenced by their WS (Zhao et al., 2022). It is essential that packaging films used to protect food items maintain their durability and remain intact despite varying environmental conditions. However, the water-insoluble nature of CHNF may diminish the water solubility properties of the packaging film. Adding anthocyanin compounds, which like water, can make the packaging film more soluble in water. However, even though they like water, the anthocyanins from butterfly pea flower extract didn't change the water solubility of these composite films much. Also, the composite film's water solubility can be greatly lowered by adding chitosan nanofiber (Zhu et al., 2023). Nanocomposite films become less soluble when ZNONPs are added. The polymer matrix can form strong hydrogen bonds with the hydroxyl groups of the nanoparticles and the matrix's hydroxyl and carboxyl groups when these nanoparticles are added. This, in turn, promotes better intermolecular interaction and greater cohesion within the polymer matrix. The inclusion of nanoparticles also causes water molecules to be too weak to break the nanofiller bond matrix (Zhu et al., 2023). The WS test results is in Table 9.

**Table 9** WS of halochromic film

Sample	The water solubility (%)	STD Deviation
G_I	47.5	± 0,52
G_II	45.4	± 0,62
G_III	45.3	± 0,53
G-Z_I	42.4	± 0,62
G-Z_II	40.5	± 0,62
G-Z_III	37.9	± 0,62
G-C_I	42.7	± 0,63
G-C_II	41.4	± 0,62
G-C_III	40.4	± 0,7
G-CZ_I	35.5	± 0,74
G-CZ_II	32.6	± 0,7
G-CZ_III	30.4	± 0,7

## Conclusion

According to the research results, the gelatine-chitosan nanofiber film with CHNF, ZnONPs, and anthocyanin nanofillers exhibited superior functional properties than the pure gelatine film. The research was conducted to analyze the influence of different additives (CHNF and ZnONPs) on the attributes of gelatine-based films. The hypothesis put forward was that the additives would enhance the water resistance, antioxidant activity, and antimicrobial activity of the films. The outcomes validated the hypothesis, revealing that the films with additives displayed reduced moisture absorption and increased antimicrobial activity compared to the films without additives. Additionally, the results indicated that the additives exhibited a collective effect, with the films containing both CHNF and ZnONPs (G-CZ) demonstrating the most optimal performance among all the film samples. The structure and spectrum of the packaging films were also affected by the additives, which was demonstrated by the variations in the FTIR spectra and the Young's modulus values. The experiment concluded that CHNF and ZnONPs enhanced the functionality of gelatine-based films significantly.

## Acknowledgments

For funding from the Ministry of Education, Culture, Research and Technology of the Republic of Indonesia, the author would like to thank him for his assistance in this research.

## Compliance with ethics guidelines

The authors declare they have no conflict of interest or financial conflicts to disclose.

This article contains no studies with human or animal subjects performed by authors.

## References

- Abebe, G. M. (2020). The role of bacterial biofilm in antibiotic resistance and food contamination. *International Journal of Microbiology*, 2020, 1705814. <https://doi.org/10.1155/2020/1705814>
- Alizadeh-Sani, M., Mohammadian, E., Rhim, J. W., & Jafari, S. M. (2020). pH-sensitive (halochromic) smart packaging films based on natural food colorants for the monitoring of food quality and safety. *Trends in Food Science and Technology*, 105(8), 93–144. <https://doi.org/10.1016/j.tifs.2020.08.014>
- Alizadeh-Sani, M., Tavassoli, M., McClements, D. J., & Hamishehkar, H. (2021). Multifunctional halochromic packaging materials: Saffron petal anthocyanin loaded-chitosan nanofiber/methyl cellulose matrices. *Food Hydrocolloids*, 111, 1–13.
- Alizadeh-Sani, M., Tavassoli, M., Mohammadian, E., Ehsani, A., Khaniki, G. J., Priyadarshi, R., & Rhim, J. W. (2021). pH-responsive color indicator films based on methylcellulose/chitosan nanofiber and barberry anthocyanins for real-time monitoring of meat freshness. *International Journal of Biological Macromolecules*, 166, 741–750. <https://doi.org/10.1016/j.ijbiomac.2020.10.231>
- Amjadi, S., Emaminia, S., Heyat Davudian, S., Pourmohammad, S., Hamishehkar, H., & Roufegarinejad, L. (2019). Preparation and characterization of gelatine-based nanocomposite containing chitosan nanofiber and ZnO nanoparticles. *Carbohydrate Polymers*, 216(3), 376–384. <https://doi.org/10.1016/j.carbpol.2019.03.062>
- Arifin, H. R., Djali, M., Nurhadi, B., & Vania, A. (2021). Study of the Physical Characteristics of Nanocomposite Films Reinforced with Zinc Oxide Nanoparticles. *Prosiding IRWNS*, 801–804. (Text in Indonesian) <https://jurnal.polban.ac.id/ojs-3.1.2/proceeding/article/view/2800/2191>
- Bahar, A., Kusumawati, N., & Catur, A. (2023). The Effect of G/CHNF/ZnONPs Packaging on Nutritional Content, Antibacterial Activity, and Shelf Life of Cheddar Cheese. *International Journal on Advanced Science Engineering Information Technologies*, 13(4), 1355–1362. <https://doi.org/10.18517/ijaseit.13.4.18531>
- Bahar, A., Samik, S., Sianita, M. M., Kusumawati, N., Khafidlah, I., Muslim, S., & Auliya, A. S. (2023). Development and Characterization of Edible Films Based on Gelatine/Chitosan Composites Incorporated with Zinc Oxide Nanoparticles for Food Protection. *Molekul*, 18(3), 339–350. <https://doi.org/10.20884/1.jm.2023.18.3.6630>
- Bari, M. A., & Kindziarski, W. B. (2018). Ambient volatile organic compounds (VOCs) in Calgary, Alberta: Sources and screening health risk assessment. *Science of the Total Environment*, 631, 627–640. <https://doi.org/10.1016/j.scitotenv.2018.03.023>
- Barman, A., De, A., & Das, M. (2020). Stabilization and Dispersion of ZnO Nanoparticles in PVA Matrix. *Journal of Inorganic and Organometallic Polymers and Materials*, 30(6), 2248–2257. <https://doi.org/10.1007/s10904-019-01395-7>
- Campos, A. de, Claro, P. C., Luchesi, B. R., Miranda, M., Souza, F. V. D., Ferreira, M. D., & Marconcini, J. M. (2019). Curaua cellulose sheets dip coated with micro and nano carnauba wax emulsions. *Cellulose*, 26(13–14), 7983–7993. <https://doi.org/10.1007/s10570-019-02637-0>
- Chen, L., Wang, W., Wang, W., & Zhang, J. (2023). Effect of Anthocyanins on Colorimetric Indicator Film Properties. *Coatings*, 13(10), 1682. <https://doi.org/10.3390/coatings13101682>
- Chen, Z., Wang, J., Wu, H., Yang, J., Wang, Y., Zhang, J., Bao, Q., Wang, M., Ma, Z., Tress, W., & Tang, Z. (2022). A Transparent Electrode Based on Solution-Processed ZnO for Organic Optoelectronic Devices. *Nature Communications*, 13(1), 1–12. <https://doi.org/10.1038/s41467-022-32010-y>
- Dodero, A., Escher, A., Bertucci, S., Castellano, M., & Lova, P. (2021). Intelligent packaging for real-time monitoring of food-quality: Current and future developments. *Applied Sciences*, 11(8). <https://doi.org/10.3390/app11083532>
- Drago, E., Campardelli, R., Pettinato, M., & Perego, P. (2020). Innovations in smart packaging concepts for food: An extensive review. *Foods*, 9(11), 1628. <https://doi.org/10.3390/foods9111628>
- Dzeikala, O., Prochon, M., Marzec, A., & Szczepanik, S. (2023). Preparation and Characterization of Gelatine-Agarose and Gelatine-Starch Blends Using Alkaline Solvent. *International Journal of Molecular Sciences*, 24(2). <https://doi.org/10.3390/ijms24021473>
- Erdem, B. G., & Kaya, S. (2022). Characterization and application of novel composite films based on soy protein isolate and sunflower oil produced using freeze drying method. *Food Chemistry*, 366(6). <https://doi.org/10.1016/j.foodchem.2021.130709>
- Ezati, P., Tajik, H., & Moradi, M. (2019). Fabrication and characterization of alizarin colorimetric indicator based on cellulose-chitosan to monitor the freshness of minced beef. *Sensors and Actuators, B: Chemical*, 285, 519–528. <https://doi.org/10.1016/j.snb.2019.01.089>
- Fernández-Marín, R., Fernandes, S. C., Sánchez, M. Á. A., & Labidi, J. (2022). Halochromic and antioxidant capacity of smart films of chitosan/chitin nanocrystals with curcuma oil and anthocyanins. *Food Hydrocolloids*, 123, 107119. <https://doi.org/10.1016/j.foodhyd.2021.107119>

- Firouz, M. S., Mohi-Alden, K., & Omid, M. (2021). A critical review on intelligent and active packaging in the food industry: Research and development. *Food Research International*, *141*, 110113. <https://doi.org/10.1016/j.foodres.2021.110113>
- Hai, L. Van, Zhai, L., Kim, H. C., Panicker, P. S., Pham, D. H., & Kim, J. (2020). Chitosan nanofiber and cellulose nanofiber blended composite applicable for active food packaging. *Nanomaterials*, *10*(9), 1–14. <https://doi.org/10.3390/nano10091752>
- Hajji, S., Kchaou, H., Bkhairia, I., Ben Slama-Ben Salem, R., Boufi, S., Debeaufort, F., & Nasri, M. (2021). Conception of active food packaging films based on crab chitosan and gelatine enriched with crustacean protein hydrolysates with improved functional and biological properties. *Food Hydrocolloids*, *116*(8). <https://doi.org/10.1016/j.foodhyd.2021.106639>
- Heidari, M., Khomeiri, M., Yousefi, H., Rafieian, M., & Kashiri, M. (2021). Chitin nanofiber-based nanocomposites containing biodegradable polymers for food packaging applications. *Journal Fur Verbraucherschutz Und Lebensmittelsicherheit*, *16*(3), 237–246. <https://doi.org/10.1007/s00003-021-01328-y>
- Huang, S., Xiong, Y., Zou, Y., Dong, Q., Ding, F., Liu, X., & Li, H. (2019). A novel colorimetric indicator based on agar incorporated with *Arnebia euchroma* root extracts for monitoring fish freshness. *Food Hydrocolloids*, *90*, 198–205. <https://doi.org/10.1016/j.foodhyd.2018.12.009>
- Javed, R., Zia, M., Naz, S., Aisida, S. O., Ain, N. U., & Ao, Q. (2020). Role of capping agents in the application of nanoparticles in biomedicine and environmental remediation: Recent trends and future prospects. *Journal of Nanobiotechnology*, *18*, 1-15. <https://doi.org/10.1186/s12951-020-00704-4>
- Jiao, X., Li, M., Cheng, Z., Yu, X., Yang, S., & Zhang, Y. (2020). Recyclable Superhydrophobic, Antimoisture-Activated Carbon Pellets for Air and Water Purification. *ACS Applied Materials and Interfaces*, *12*(22), 25345–25352. <https://doi.org/10.1021/acsami.0c06274>
- Kang, S., Wang, H., Xia, L., Chen, M., Li, L., Cheng, J., Li, X., & Jiang, S. (2020). Colorimetric film based on polyvinyl alcohol/okra mucilage polysaccharide incorporated with rose anthocyanins for shrimp freshness monitoring. *Carbohydrate Polymers*, *229*, 115402. <https://doi.org/10.1016/j.carbpol.2019.115402>
- Long, J., Zhang, W., Zhao, M., & Ruan, C. Q. (2023). The reduce of water vapor permeability of polysaccharide-based films in food packaging: A comprehensive review. *Carbohydrate Polymers*, *321*(6), 121267. <https://doi.org/10.1016/j.carbpol.2023.121267>
- Lu, M., Zhou, Q., Yu, H., Chen, X., & Yuan, G. (2022). Colorimetric indicator based on chitosan/gelatine with nano-ZnO and black peanut seed coat anthocyanins for application in intelligent packaging. *Food Research International*, *160*, 111664. <https://doi.org/10.1016/j.foodres.2022.111664>
- Luo, Q., Hossen, M. A., Zeng, Y., Dai, J., Li, S., Qin, W., & Liu, Y. (2022). Gelatine-based composite films and their application in food packaging: A review. *Journal of Food Engineering*, *313*, 110762. <https://doi.org/10.1016/j.jfoodeng.2021.110762>
- Ma, S., Zheng, Y., Zhou, R., & Ma, M. (2021). Characterization of chitosan films incorporated with different substances of konjac glucomannan, cassava starch, maltodextrin and gelatine, and application in mongolian cheese packaging. *Coatings*, *11*(1), 84. <https://doi.org/10.3390/coatings11010084>
- Martiana, A., Arief, I. I., Nuraini, H., & Taufik, E. (2020). The Quality of Bali Beef from East Nusa Tenggara during Distribution Process from Slaughterhouse to Consumers. *Jurnal Ilmu Produksi Dan Teknologi Hasil Peternakan*, *8*(1), 8–14. <https://doi.org/10.29244/jipthp.8.1.8-14>
- Mohammed, M., Oleiwi, J. K., Jawad, A. J. afar M., Mohammed, A. M., Osman, A. F., Rahman, R., Adam, T., Betar, B. O., Gopinath, S. C. B., & Dahham, O. S. (2023). Effect of zinc oxide surface treatment concentration and nanofiller loading on the flexural properties of unsaturated polyester/kenaf nanocomposites. *Heliyon*, *9*(9), e20051. <https://doi.org/10.1016/j.heliyon.2023.e20051>
- Moustafa, H., Youssef, A. M., Darwish, N. A., & Abou-Kandil, A. I. (2019). Eco-friendly polymer composites for green packaging: Future vision and challenges. *Composites Part B: Engineering*, *172*(5), 16–25. <https://doi.org/10.1016/j.compositesb.2019.05.048>
- Musso, Y. S., Salgado, P. R., & Mauri, A. N. (2019). Smart gelatine films prepared using red cabbage (*Brassica oleracea* L.) extracts as solvent. *Food Hydrocolloids*, *89*(11), 674–681. <https://doi.org/10.1016/j.foodhyd.2018.11.036>
- Nandiwilastio, N., Muchtadi, T. R., Suyatma, N. E., & Yuliani, S. (2019). Effect of Beeswax and Zinc Oxide Nanoparticles Addition on the Physical and Mechanical Properties of Chitosan-Based Films. *Jurnal Teknologi dan Industri Pangan*, *30*(2), 119–126. (Text in Indonesian) <https://doi.org/10.6066/jtip.2019.30.2.119>
- Othman, S. H., Kahar, N. S., Nordin, N., Alyas, N. D., Hasnan, N. Z. N., Talib, R. A., & Karyadi, J. N. W. (2023). Tapioca starch-based films containing oregano, Vietnamese mint, and curry leaf essential oils for food packaging applications. *International Food Research Journal*, *30*(2), 497–513. <https://doi.org/10.47836/ifrj.30.2.19>

- Qian, M., Liu, D., Zhang, X., Yin, Z., Ismail, B. B., Ye, X., & Guo, M. (2021). A review of active packaging in bakery products: Applications and future trends. *Trends in Food Science and Technology*, 114(6), 459–471. <https://doi.org/10.1016/j.tifs.2021.06.009>
- Rahman, M. M., Islam, M. S., & Li, G. S. (2018). Development of PLA/CS/ZnO nanocomposites and optimization its mechanical, thermal and water absorption properties. *Polymer Testing*, 68, 302–308. <https://doi.org/10.1016/j.polymertesting.2018.04.026>
- Roy, S., Biswas, D., & Rhim, J. W. (2022). Gelatine/Cellulose Nanofiber-Based Functional Nanocomposite Film Incorporated with Zinc Oxide Nanoparticles. *Journal of Composites Science*, 6(8), 1–11. <https://doi.org/10.3390/jcs6080223>
- Roy, S., Kim, H. J., & Rhim, J. W. (2021). Effect of blended colorants of anthocyanin and shikonin on carboxymethyl cellulose/agar-based smart packaging film. *International Journal of Biological Macromolecules*, 183, 305–315. <https://doi.org/10.1016/j.ijbiomac.2021.04.162>
- Roy, S., & Priyadarshi, R. (2021). Composite Films Reinforced with ZnO Nanoparticles and Propolis for Meat Packaging Applications. *Foods*, 10(2789). <https://doi.org/10.3390/foods10112789>
- Sahraee, S., Milani, J. M., Ghanbarzadeh, B., & Hamishehkar, H. (2017). Physicochemical and antifungal properties of bio-nanocomposite film based on gelatine-chitin nanoparticles. *International Journal of Biological Macromolecules*, 97(12), 373–381. <https://doi.org/10.1016/j.ijbiomac.2016.12.066>
- Saliu, F., & Della Pergola, R. (2018). Carbon dioxide colorimetric indicators for food packaging application: Applicability of anthocyanin and poly-lysine mixtures. *Sensors and Actuators B: Chemical*, 258, 1117–1124. <https://doi.org/10.1016/j.snb.2017.12.007>
- Shahmohammadi, F., & Almasi, H. (2016). Morphological, physical, antimicrobial and release properties of ZnO nanoparticles-loaded bacterial cellulose films. *Carbohydrate Polymers*, 149, 8–19. <https://doi.org/10.1016/j.carbpol.2016.04.089>
- Sharaby, M. R., Soliman, E. A., & Khalil, R. (2024). Halochromic smart packaging film based on montmorillonite/polyvinyl alcohol-high amylose starch nanocomposite for monitoring chicken meat freshness. *International Journal of Biological Macromolecules*, 258(6), 128910. <https://doi.org/10.1016/j.ijbiomac.2023.128910>

- Sitanggang, A. B., Irsali, M. F., & Rawdkeun, S. (2020). Incorporation of Oleate and Anthocyanin Extract into Gelatin Films as a pH Indicator for Smart Packaging. *Jurnal Teknologi Dan Industri Pangan*, 31(1), 66–75. <https://doi.org/10.6066/jtip.2020.31.1.66>
- Soradech, S., Nunthanid, J., Limmatvapirat, S., & Luangtana-anan, M. (2017). Utilization of shellac and gelatine composite film for coating to extend the shelf life of banana. *Food Control*, 73, 1310–1317. <https://doi.org/10.1016/j.foodcont.2016.10.059>
- Wang, S., Xia, P., Wang, S., Liang, J., Sun, Y., Yue, P., & Gao, X. (2019). Packaging films formulated with gelatine and anthocyanins nanocomplexes: Physical properties, antioxidant activity and its application for olive oil protection. *Food Hydrocolloids*, 96. <https://doi.org/10.1016/j.foodhyd.2019.06.004>
- Yong, H., Wang, X., Zhang, X., Liu, Y., Qin, Y., & Liu, J. (2019). Effects of anthocyanin-rich purple and black eggplant extracts on the physical, antioxidant and pH-sensitive properties of chitosan film. *Food Hydrocolloids*, 94, 93–104. <https://doi.org/10.1016/j.foodhyd.2019.03.012>
- Zhang, P., Li, Y., Chong, S., Yan, S., Yu, R., Chen, R., Si, J., & Zhang, X. (2022). Identification and quantitative analysis of anthocyanins composition and their stability from different strains of *Hibiscus syriacus* L. flowers. *Industrial Crops and Products*, 177(6), 114457. <https://doi.org/10.1016/j.indcrop.2021.114457>
- Zhang, X., Zhao, Y., Li, Y., Zhu, L., Fang, Z., & Shi, Q. (2020). Physicochemical, mechanical and structural properties of composite edible films based on whey protein isolate/psyllium seed gum. *International Journal of Biological Macromolecules*, 153, 892–901. <https://doi.org/10.1016/j.ijbiomac.2020.03.018>
- Zhao, L., Liu, Y., Zhao, L., & Wang, Y. (2022). Anthocyanin-based pH-sensitive smart packaging films for monitoring food freshness. *Journal of Agriculture and Food Research*, 9(6), 100340. <https://doi.org/10.1016/j.jafr.2022.100340>
- Zhu, B., Zhong, Y., Wang, D., & Deng, Y. (2023). Active and Intelligent Biodegradable Packaging Based on Anthocyanins for Preserving and Monitoring Protein-Rich Foods. *Foods*, 12(24), 4491. <https://doi.org/10.3390/foods12244491>
- Zulkiflee, I., & Fauzi, M. B. (2021). Gelatine-polyvinyl alcohol film for tissue engineering: A concise review. *Biomedicines*, 9(8), 979. <https://doi.org/10.3390/biomedicines9080979>